POS2-19

Measured electrical characteristics of an array feed offset parabolic reflector antenna

Junichi Shinohara[1], Naobumi Michishita[1],Yoshihide Yamada[1],
Mohammad Tariqul Islam[2] and Norbahiah Misran[2]
[1]National Defense Academy, 1-10-20 Hashirimizu, Yokosuka, Japan, yyamada@nda.ac.jp
[2]Universiti Kebangsaan Malaysia, 43600 Bangi, Selangor Darul Ehsan, Malaysia tariqul@ukm.my

1. Introduction

For convenient portable earth stations of satellite communications, offset parabolic reflector antennas are employed in broadcasting TV [1] and military uses [2]. Authors have been developing an array feed offset parabolic reflector antenna [3]. The array feed was designed to improve antenna gain of the reflector antenna [4]. Realization of the array feed was ensured through electromagnetic simulations [5]. In this paper, measured electrical characteristics of a fabricated array feed and the offset parabolic reflector antenna. Through comparisons of measured and calculated results, actual realization of the antenna and effectiveness of radiation pattern synthesis of the array feed are ensured.

2. Outlines of the antenna performances

The antenna configuration is shown in Fig.1. An offset parabolic reflector is illuminated by an array feed. The radiation pattern of the array feed is synthesized in order to achieve an uniform illumination distribution on the aperture plane. In fig.2, a configuration of the array feed is shown. The array is composed of 3×6 micro strip patch antennas. At the column array, excitation coefficients of 6 array elements are determined as a result of array radiation pattern synthesis by the least mean square method.

3. Measured electrical characteristics of the array feed

3.1 Designed date of excitation coefficients

Calculated results of current distributions on the designed array feed are shown in Fig.3. The feature of this configuration is that the feed point is concentrated at one point. In order to achieve this configuration, feeding circuit is adequately designed. Array element patch sizes, separations, excitation coefficients and feed circuit are determined at 11 GHz. However, reflection coefficient becomes minimum value at 10.6 GHz as shown in Fig.7. Current distributions are obtained at 10.6 GHz. As for feed loss of this structure, ohmic loss and dielectric loss are estimated. First, radiation electric fields are compared with copper conductor and perfect conductor. The ohmic loss is estimated 0.1 dB. Next, in the case of $\tan\delta = 0.0018$ and $\tan\delta = 0$, dielectric loss is estimated 0.1 dB. As a result, this feed structure can achieve very small losses. Calculated excitation amplitudes and phases are shown in Fig.4 and Fig.5, respectively. In these figures, results in one to three column elements are shown. At all columns, excitation amplitudes and phases agree very well with the design objectives.

3.2 Fabrication and measured results

The fabricated array feed is shown in Fig.6. Feed circuit and patches are shaped by a cutting machine on a Teflon substrate of 0.8 mm thickness. Measured and calculated reflection coefficients are shown in Fig.7. The difference of the minimum frequency is caused by the difference of dielectric constant at the actual substrate. Excellent low reflection coefficient is achieved in rather wide frequencies of 10 % band width. Measured and calculated radiation patterns are shown in Fig.8. In the column direction of Fig.8 (a), measured and calculated results agree very well. Maximum electric field level becomes 12.2 dBi. This value corresponds to the antenna efficiency of

94.4 %. Sidelobes become approximately −10 dB. These sideloves may cause large spillover from the reflector. Through this agreement, achievements of accurate excitation coefficients are ensured. In the row direction of Fig.8 (b), the measured pattern becomes broader than the calculated pattern. This pattern degradation may be produced by the achieved phase difference between column arrays. Fabrication method of the feed circuits between the columns should be reconsidered.

4. Measured results of the antenna

Configuration of the fabricated offset parabolic reflector antenna is shown in Fig.9. The reflector is fabricated with a carbon FRP material. The array feed works at a horizontal polarization. Radiation angles are denoted by θ and ϕ. The main beam exists in the x axis direction that corresponds to $\theta = 90°$. First of all, electric near field distributions of an array feed offset reflector are calculated and is shown in Fig.10. It is seen that radiation electric fields from the array feed are well concentrated in the reflector region. As for reflected electric fields from the reflector, the electric field intensity on a plane wave becomes almost constant over the aperture plane whose diameter is 248 mm. The effect of radiation pattern synthesis is ensured through the uniform intensity of the plane wave. At the upper and lower edges of the reflector, appreciable spill over levels are observed. Measured radiation patterns are shown in Fig.11 and Fig.12. Fig.11 shows the results in the zx plane. In the near axis radiation pattern of Fig.11 (a), measured and calculated results agree very well. The half power beam width becomes $\theta_{BV} = 6.8°$. Rather low sidelobe levels less than −20 dB are achieved. Measured antenna gain of 26.0 dBi is obtained by comparing receiver levels of measured antenna and standard gain antenna whose gain is 20.0 dBi. The calculated antenna gain of 26.4 dBi corresponds to antenna efficiency of $\eta = 74.4\%$. In Fig.11 (b), wide angle radiation patterns are shown. Receiver levels are saturated at −10 dBi. Around the zenith direction ($\theta = 0°$) and reflector backward direction ($\theta = -90°$), appreciable spillover levels are observed. In Figure.12, radiation patterns in the xy plane are shown. In the near axis radiation pattern of Fig.12 (a), the main beam shape agrees well between measured and calculated results. The half power beam width becomes $\theta_{BH} = 6.7°$. Measured sideloves become larger than calculated levels more than 5 dB. The reason of these increase are the edge level increases of the reflector that is shown in Fig.8 (b). In the wide angle radiation pattern of Fig.12 (b), measured levels are saturated at −5 dBi. Therefore, very low sidelobe characteristics of calculated results are not ensured in this measurement.

5. Conclusion

The array feed performances and total antenna radiation characteristics are confirmed through measurement. Because the array feed circuit is adequately designed, very low feed loss is achieved. And antenna efficiency of $\eta = 74.4\%$ is achieved. Effectiveness of the radiation pattern synthesis at the array feed is ensured.

References

[1] K. Miwa, M. Tanaka, T. Naito, and Y. Endo, “A New FRP Parabolic Antenna for Satellite Broadcasting System, ” ITE Technical Report, vol.8, no.7, pp.7-12, May. 1984.

[2] http://www42.tok2.com/home/fleet7/FilmScanner/NegaScanJGSDFe. html, antennas of TASCOM －X

[3] J. Shinohara, N. Michishita, Y. Yamada, M. Tariqul Islam and N. Misran, “Design of array feed offset parabolic reflector antenna for a simple earth station” International Conference on Space science and Communication, July. 2011.

[4] J. Shinohara, N. Michishita, Y. Yamada, M. Tariqul Islam and N. Misran, “Simulation Results of a Dual Band and Shaped Beam Array Feed for an Offset Parabolic Reflector,” International Symposium on Antennas and Propagation, October. 2011.

[5] J. Shinohara, N. Michishita, Y. Yamada, M. Tariqul Islam and N. Misran, “Achievement of a Shaped Beam Array Feed for an Offset Parabolic Reflector,” ACES’12, pp.786-789, April 2012

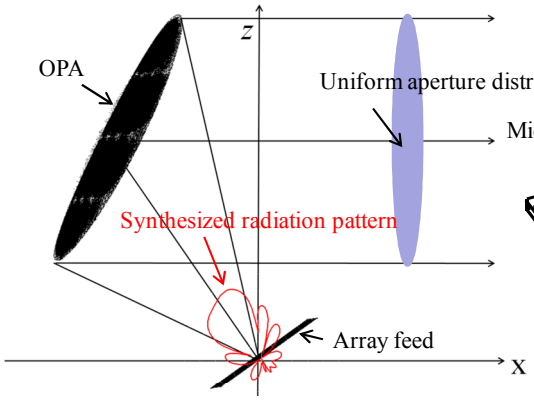

Figure 1: Antenna configuration

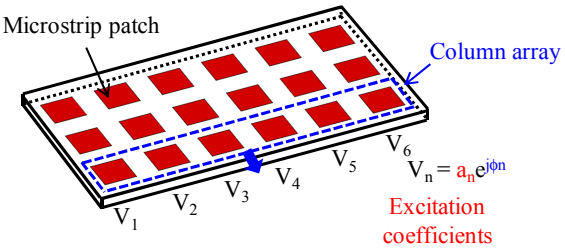

Figure 2: Configuration of array feed

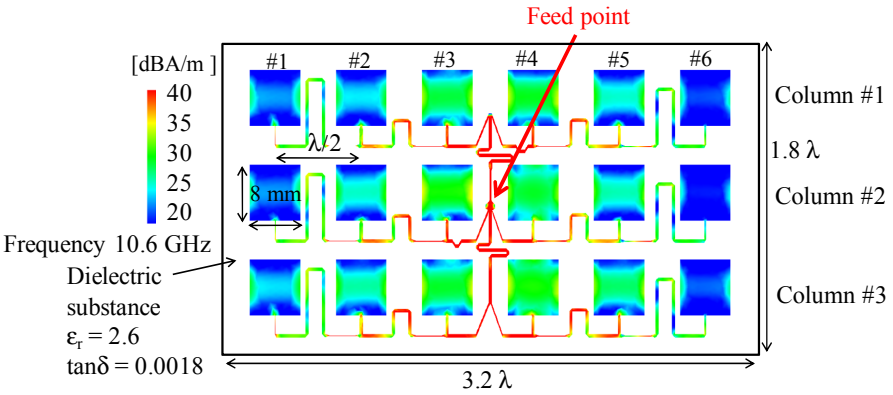

Figure 3: Series feed configuration and achieved current distribution

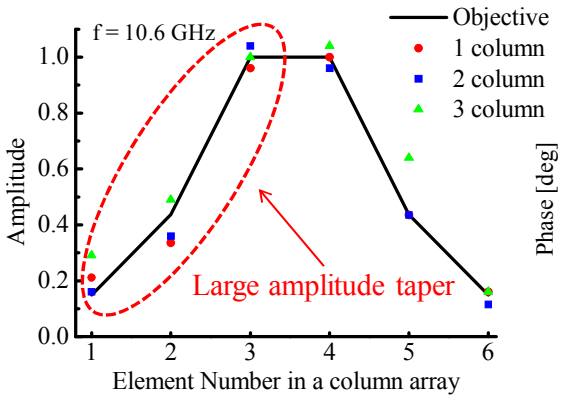

Figure 4: Amplitude of excitation coefficients

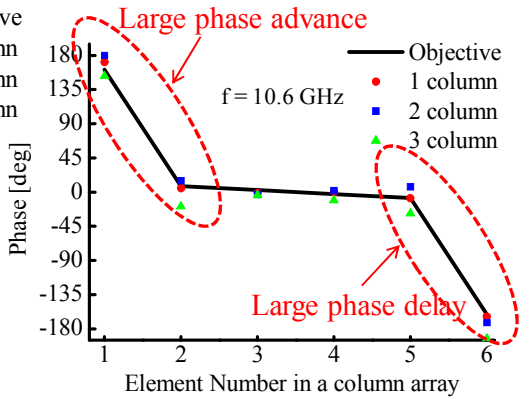

Figure 5: Phase of excitation coefficients

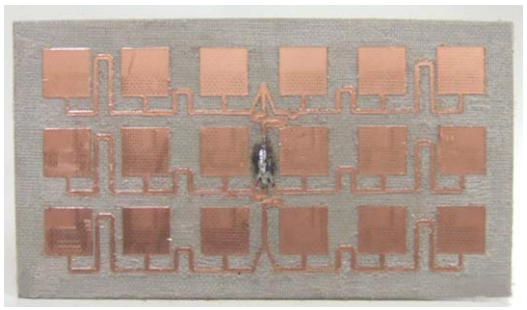

Figure 6: Fabricated array feed

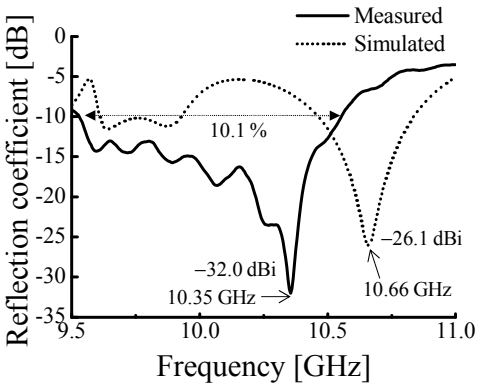

Figure 7: Reflection coefficient

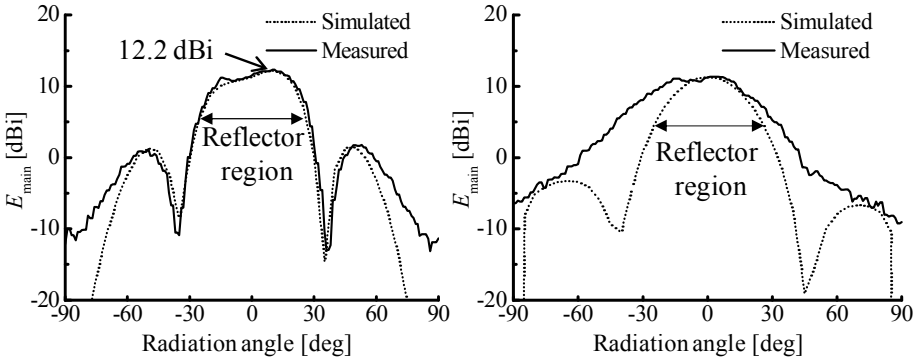

(a) Column direction (b) Row direction

Figure 8: Radiation patterns of the fabricated array

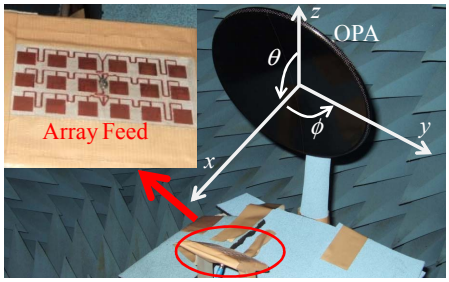

Figure 9: Antenna measurement configuration

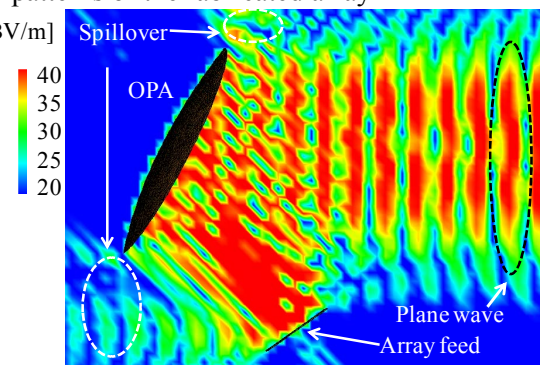

Figure 10: Electric near field distribution

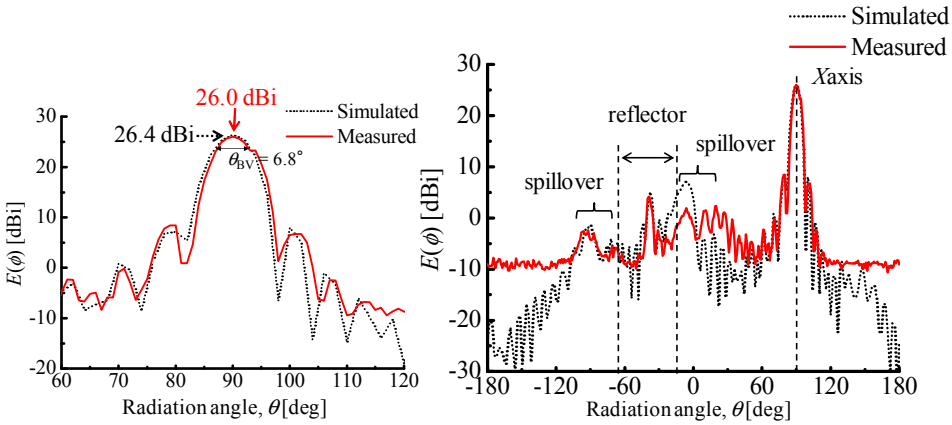

(a) Near axis radiation pattern (b) Wide angle radiation pattern

Figure 11: Radiation pattern in the *zx*–plane

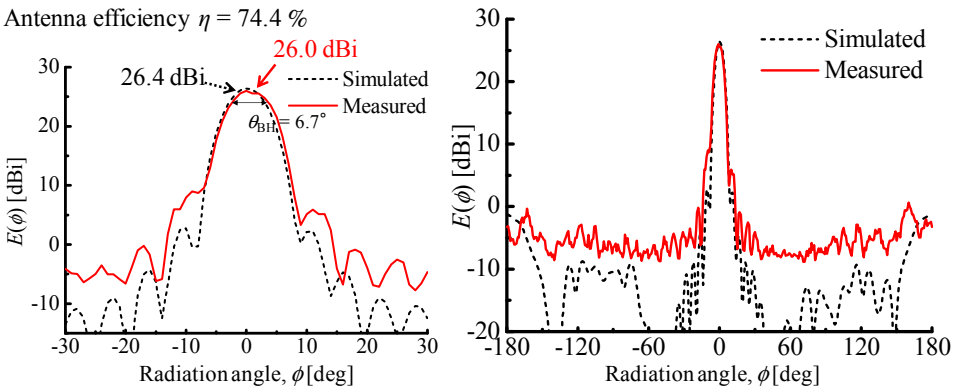

(a) Near axis radiation pattern (b) Wide angle radiation pattern

Figure 12: Radiation pattern in the *xy*–plane